Research Square

Preprints are preliminary reports that have not undergone peer review.
They should not be considered conclusive, used to inform clinical practice,
or referenced by the media as validated information.

Tetraphenylethylene-Based Fluorescent Conjugated Microporous Polymers For Fluorescent Sensing Trinitrophenol

Liying Ren
Anqing Medical College
Xue-Chun Fang
Anqing Normal University
Feng-Qiang Wang
Anqing Normal University
Tongmou Geng (2318052317@qq.com)
Anqing Normal University https://orcid.org/0000-0003-3473-8268

Research Article

Keywords: Conjugated microporous polymer, Fluorescence sensor, Trinitrophenol, Tetraphenylethylene, Dinitrophenol

Posted Date: September 20th, 2021

DOI: https://doi.org/10.21203/rs.3.rs-837543/v1

License: This work is licensed under a Creative Commons Attribution 4.0 International License.
Read Full License

Abstract

Two tetraphenylethylene-based fluorescent conjugated microporous polymers (TTTPT and TTDAT) were obtained by the Friedel–Crafts polymerization reactions catalyzed by CH_3SO_3H. In virtue of containing tetraphenylethylene, triphenylamine and s-triazine units in their porous skeletons, the resulting TTTPT and TTDAT show excellent fluorescence sensing performance for trinitrophenol with high quenching coefficients of 9.13×10^3 and 1.31×10^5 L mol^{-1}, respectively. TTDAT can also sense to dinitrophenol with the Ksv of 2.70×10^4 L mol^{-1}. The fluorescent quenching mechanisms of TTTPT and TTDAT for selective detecting TNP attribute to conventional photoinduced electron-transfer mechanism and/or the resonant energy transfer mechanism.

Introduction

As one of nitro-aromatic compounds (NACs), 2,4,6-trinitrophenol (Note it as TNP) is a significant threaten human health and national homeland safety [1]. TNP is not only one of the most dangerous explosives, but also severe environmental pollutants, and its extensive applications can cause hurt to the human body [2]. TNP can cause intense skin and eye irritation, severe respiratory disorders, liver or kidney damage, dizziness, as well as mutagenic effects, which gives rise to significant menaces to mankind health [2–5]. It is also the cause of sycosis, anaemia, gastritis, cancer, infertility and diarrhoea [5]. Because the frequent use of TNP in fireworks, dyes, leather and textile industries, a fungicide in agricultural, a powerful explosive in landmines and pharmaceutical industries, TNP unavoidably leads to its release to the environment in the process of production and utilization and brings about increased pollution of farmland and water bodies [3, 4, 6]. As it is characterized by high water-soluble, strong toxicity and low biodegradability, which can cause serious pollution to the supply of irrigation land and groundwater, and has a harmful impact on human health, TNP has already been placed at the forefront pollutants [4, 6]. Moreover, TNP has been considered an extremely dangerous explosive compared with other NACs, because of its low safety factor and high explosive energy [3, 5, 6]. Hence, fast, sensitive and selective detecting TNP is important [3–6].

Among the various TNP determination methods, for instance, gas chromatography, liquid chromatography, masss pectrometry, Raman spectroscopy, cyclic voltammetry, ion mobility spectroscopy, ion mobility spectrometry, field-effect transistor and fluorescence spectroscopy [1, 5–8], fluorescence sensing technique provides intriguing merits, for example, simplicity, excellent sensitivity, rapid response time, inexpensiveness, and it can test whether in solution or in solid-phase [3, 5–10].

Several electron-rich conjugated microporous polymers (CMPs) have been successfully prepared and reported as chemosensors. In particular, fluorescent CMPs have been widely used in the study of NACs detection [7, 10]. The microporous environment of the framework enables rapid diffusion of analytes, thus decreasing response time. The effective host-object interactions are valid to improve sensitivity [11]. The extended π-conjugate in CMPs can amplify signal transduction, hence further improving the sensitivity, which is known as the ‘molecular wire effect’ created by Swager group [5, 9]. Furthermore,

commercial NACs, for instance, TNP or DNP, all have the electron-withdrawing nitryl ($-NO_2$) that can interact with electron-donating CMPs, leading to effective excitation migration within the CMP porous structures to improve quenching sensitivity. Therefore, these conjugated and porous features of the organic frameworks make CMPs suitable for detecting the NACs [8, 9, 12].

Our group have developed two CMPs with the units of 1,3,5-triazine, triphenylamine (TPA) and tetraphenylethylene (TPE) (TTTPT and TTDAT, Scheme 1). TTTPT and TTDAT have the excellent porosity (564.8 and 44.1 $m^2 g^{-1}$) (Table S1), high thermal stability (575 and 487 ^oC) and excellent performances for fluorescence sensing and adsorping I_2 [13]. As a continuation of the work, we studied the fluorescence sensing properties of TTTPT and TTDAT for TNP and DNP in the contribution.

Results And Discussion

2.1. Fluorescence response time

When TTTPT and TTDAT were dispersed in some ordinary solvents, they emitted strong fluorescence. TTTPT dispersion in 1,4-dioxane (DOX) showed the most robust fluorescence under light excitation at 460 nm wavelength, while TTDAT dispersion in DMF emitted the maximum fluorescence upon excitation at 350 nm [13]. Therefore, we studied the relationships between fluorescence intensities of TTTPT dispersion in DOX and TTDAT dispersion in DMF (1.0 mg mL^{-1}) and the time after addition of TNP (5.0×10^{-4} and 2.5×10^{-5} mol L^{-1}) (Fig. 1). The fluorescence of TTTPT and TTDAT decreased almost instantly, and reached the quenching equilibrium in less than 20 s, which indicated that the porous networks and extended conjugate structure have fast responses to TNP [14, 15].

2.2. Sensitivity of the CMPs

Since TTTPT and TTDAT are porous and fluorescent, we then investigated their chemosensing behaviour by choosing the NACs, including TNP, p-nitrophenol (p-NP), 4-nitrotoluene (p-NT), nitrobenzene (NB), 2,4-dinitrotoluene (DNT), paradinitrobenzene (p-DNB), m-nitrobenzene (m-DNB), 3-nitrophenol (m-NP), 2,4-dinitrotoluene (DNT), and DNP, as well as phenol (PhOH). Among them, the most toxic and damaging compounds, TNP and DNP, should be deserve particular attention [16]. Figure 2a-c showed the fluorescence spectra of TTTPT and TTDAT with the incremental addition of different amounts of TNP and DNP into the dispersions of TTTPT in DOX and TTDAT in DMF. Apparently, the fluorescence of TTTPT and TTDAT was quenched when TNP was gradually added into the dispersions. When other NACs were gradually added into the dispersion, respectively, the quenching efficiencies were very low, indicating that TTTPT and TTDAT have good selectivity for TNP over other NACs [1, 16, 17]. We used the Stern–Volmer equation, $(I_0/I) = K_{SV}[A] + 1$, to calculate the quenching coefficients (or Stern–Volmer constants, K_{SV}) of TNP [16, 18]. According to the Stern-Volmer curves, the Ksv values of TTTPT and TTDAT were estimated to be 9.13×10^3 and 1.31×10^5 L mol^{-1}, respectively (Fig. 2d and Fig. 2e, Table 1), which are much bigger than those for other NACs (Table S2 ESI†). Fluorescence spectrometric titration experiments proved that TTDAT can fluorescent sense DNP and has high sensitivity, and its Ksv reaches 2.70×10^4 L

mol^{-1}. The detection limits (LODs) of TNP in DOX for TTTPT and in DMF for TTDAT are severally 1.15×10^{-13} and 5.56×10^{-13} mol L^{-1} (Table 1). The LOD of DNP in DMF for TTDAT was determined to be 5.56×10^{-13} mol L^{-1}. These results showed that of TTTPT and TTDAT in dispersions possess the high sensitivity for TNP and DNP detection and are comparable to other CMPs (Table S2) [1, 16, 17, 19].

Table 1
The equation of I_0/I of TTTPT and TTDAT to the concentrations of TNP and DNP for suspension in DOX and DMF.

CMPs	Solvent	The equation	Regression coefficient (R)	The concentration range (mol L^{-1})	LODs (mol L^{-1})
TTTPT	DOX	$I_0/I = 0.9065 + 9.13\times10^3[PA]$	0.9968	$1.0\times10^{-5}$to 7.0×10^{-4}	1.64×10^{-11}
TTDAT	DMF	$I_0/I = 0.9302 + 1.31\times10^5[PA]$	0.9834	0 to 1.0×10^{-5}	1.15×10^{-13}
TTDAT	DMF	$I_0/I = 0.9904 + 2.70\times10^4[DNP]$	0.9966	0 to 1.5×10^{-5}	5.56×10^{-13}

2.3. Selectivity and competitiveness experiments for TNP detection

The sensing selectivities of TTTPT and TTDAT systems to TNP were investigated (Fig. 3, Red bar). 5.0×10^{-4} and 2.5×10^{-5} mol L^{-1} NACs (p-NP, TNP, NB, p-NT, o-NP, p-DNB, DNT, m-DNB, m-NP, and DNP) and PhOH were added to TTTPT and TTDAT dispersions, respectively. The fluorescence of TTTPT and TTDAT was strongly quenched by TNP. In contrast, fluorescence intensities of TTTPT and TTDAT were not obvious changes after other NACs and PhOH added. The results indicated that TTTPT and TTDAT are well selective for detecting TNP [1, 20–22].

In order to check the selectivity of TTTPT and TTDAT for the actual detection of TNP, the competitive experiments were actualized in the presence of the various competitive NACs and PhOH with a concentration of 5.0×10^{-4} and 2.5×10^{-5} mol L^{-1} for the dispersions of TTTPT and TTDAT, respectively. The changes of fluorescence intensities of TTTPT and TTDAT were monitored upon addition of TNP in the presence of other NACs and PhOH. As is seen from Fig. 3 (Green bar), neither of the other NACs nor PhOH have no interference with TTTPT detecting TNP except to DNP. Similarly, the anti-interference of TTDAT toward TNP was further validated. The results further showed that TTTPT and TTDAT are well selective for detecting TNP, indicating that the fluorescence intensities of TTTPT or TTDAT were slightly affected by the addition of other NACs and PhOH, and TTTPT and TTDAT dispersions have the excellent anti-interference ability [1, 6].

2.4. The quenching mechanism

The S–V plots are non-linear with the the concentrations of TNP and DNP increasing, (Fig. 2c), indicating that a resonant energy transfer mechanism exists during quenching, and the static quenching processes coexists synchronously with the dynamical quenching processes during the detecting processes [6, 9, 23].

In order to comprehend the cause of the TTTPT or TTDAT selectivity to TNP, we measured the UV-Vis spectra of NACs and PhOH and compared them with the fluorescence spectra of the two CMPs, and employed the resonance energy transfer (RET) and photoinduced electron transfer (PET) mechanisms to explain the sensing mechanisms [6, 20]. Except for DNP, the UV-Vis spectra of NACs and PhOH hardly overlap the fluorescence spectrum of TTTPT, implying that there is no the RET process happening in the sensing process (Fig. 4a). As shown in Fig. 4b, there are overlaps among TNP, DNP, DNT, m-NP, p-NP and o-NP with TTTPT, which showed that there are energy transfer among TTDAT with TNP, DNP, DNT, m-NP, p-NP and o-NP (Fig. 4b) [20].

If the lowest unoccupied molecular orbital (LUMO) energy levels of the CMPs are higher than that of the analytes, the exciting electrons will transfer from CMPs to the analytes, and then perform fluorescence quenching, which is the PET quenching pathway [20]. Therefore, the HOMO and LUMO energy levels of TTTPT, TTDAT, the NACs and PhOH had been calculated (Fig. 5 and Table S3). The LUMO energy levels of TTTPT or TTDAT are lower than these of NB, p-NT and PhOH, which would hinder the radiative transition from TTTPT or TTDAT to NB, p-NT and PhOH, thus, there is no effective fluorescence quenching [8, 19, 20]. The LUMO energy levels of the TTTPT or TTDAT are higher than those of some NACs (such as TNP, p-DNB, DNP, m-DNB, o-NP, and DNT), which promotes the electrons transferring from TTTPT or TTDAT to electron-deficient NACs, and causes the fluorescence quenching phenomenon [9, 16, 20, 22, 24] (Fig. 5). Because the LUMO energy level of TNP is very lower than those of the other NACs and PhOH, TNP can quench more efficiently the fluorescence of TTTPT or TTDAT than other NACs and PhOH [22].

Conclusion

The fluorescent tetraphenylethylene-based conjugated microporous polymers containing triphenylamine and s-triazine units (TTTPT and TTDAT) were successfully used for fluorescence sensing trinitrophenol and dinitrophenol. Both TTTPT and TTDAT have the high sensitivity for trinitrophenol with quenching constants (Ksv) of 9.13×10^3 and 1.31×10^5 L mol^{-1}. TTTPT can also sense dinitrophenol with the Ksv of 2.70×10^4 L mol^{-1}. The fluorescent quenching mechanisms of TTTPT and TTDAT for selective detecting TNP were also studied by experiments and theoretical calculations, which could attribute to the conventional photoinduced electron-transfer mechanism and, or the resonant energy transfer mechanism.

Declarations

Author Declarations

We wish to draw the attention of the Editor to the following facts which may be considered aspotential conflicts of interest and to significant financial contributions to this work.

-Funding (information that explains whether and by whom the research was supported)

This work was supported by Natural Science Foundation of Anhui Education Department (under Grant No. KJ2020A0887 and KJ2018A0319), Youth Talent Fund Key Projects of Anhui Education Department (under Grant No. gxyqZD2019114), and the Open Fund of AnHui Province Key Laboratory of Optoelectronic and Magnetism Functional Materials supported (under Grant No. ZD2021001).

-Conflicts of interest/Competing interests (include appropriate disclosures)

The authors declare that they have no known competing financial interests or personal relationships that could have appeared to influence the work reported in this paper.

-Ethics approval/declarations (include appropriate approvals or waivers)

We further confirm that any aspect of the work covered in this manuscript that has involved either experimental animals or human patients has been conducted with the ethical approval of all relevant bodies and that such approvals are acknowledged within the manuscript.

-Consent to participate (include appropriate statements)

We confirm that the manuscript has been read and approved by all named authors and that there are no other persons who satisfied the criteria for authorship but are not listed. We further confirm that the order of authors listed in the manuscript has been approved by all of us.

-Consent for publication (include appropriate statements)

We confirm that we have given due consideration to the protection of intellectual property associated with this work and that there are no impediments to publication, including the timing of publication, with respect to intellectual property. In so doing we confirm that we have followed the regulations of our institutions concerning intellectual property.

-Availability of data and material/ Data availability (data transparency, if link please provide the link to access. For further information, go to -https://www.springernature.com/gp/authors/research-data-policy/data-availability-statements/12330880)

We understand that the Corresponding Author is the sole contact for the Editorial process (including Editorial Manager and direct communications with the office). He/she is responsible for communicating with the other authors about progress, submissions of revisions and final approval of proofs. We confirm that we have provided a current, correct email address which is accessible by the Corresponding Author and which has been configured to accept email from gengtongmou@sina.com.cn

-Code availability (software application or custom code)

There is not applicable' forCode availability (software application or custom code).

-Authors' contributions (all authors should be individually mentioned in the author contribution statement. Please represent authors' names using their full initials, starting with the first name initial followed by the surname. Example: ABC edited the draft for general write up, DEF participated in mathematical design of the proposed method etc.)

The authors contributed as follows:

Liying Ren: Investigation, Operation in experiment.

Xuechun Fang: Investigation, Operation in experiment, Data handling.

Fengqiang Wang: Investigation, Operation in experiment, Software.

Tongmou Geng: Conceptualization, Methodology, Software, Resources, Supervision, Writing- Original Draft, Writing- Reviewing and Editing.

Signed by all authors as follows:

Liying Ren: Anqing Medical and Pharmaceutical College, August 24, 2021

Xuechun Fang: Anqing Normal University, August 24, 2021

Fengqiang Wang: Anqing Normal University, August 24, 2021

Tongmou Geng: Anqing Normal University, August 24, 2021

References

1. Li WT, Hu ZJ, Meng J, Zhang X, Gao W, Chen ML, Wang JH (2021) Zn-based metal organic framework-covalent organic framework composites for trace lead extraction and fluorescence detection of TNP. J Hazard Materi 411:125021. 10.1016/j.jhazmat.2020.125021
2. Wang M, Zhang HT, Guo L, Cao DP (2018) Fluorescent polymer nanotubes as bifunctional materials for selective sensing and fast removal of picric acid. Sensor Actuat B-Chem 274:102–109. 10.1016/j.snb.2018.07.132
3. Wang K, Wang WJ, Pan SH, Fu YM, Dong B, Wang H (2020) Fluorescent self-propelled covalent organic framework as a microsensor for nitro explosive detection. Appl Mater Today 19:100550. 10.1016/j.apmt.2019.100550
4. Wang M, Gao MJ, Deng LL, Kang X, Zhang KL, Fu QF, Xia ZN, Gao D (2020) A sensitive and selective fluorescent sensor for 2,4,6-trinitrophenol detection based on the composite material of magnetic

covalent organic frameworks, molecularly imprinted polymers and carbon dots. Microchem J 154:104590. 10.1016/j.microc.2019.104590

5. Kaleeswara D, Murugavel R (2018) Picric acid sensing and CO_2 capture by a sterically encumbered azo-linked fluorescent triphenylbenzene based covalent organic polymer. J Chem Sci 130:1. 10.1007/s12039-017-1403-2
6. Jiang N, Li GF, Che WL, Zhu DX, Su ZM, Bryce MR (2018) Polyurethane derivatives for highly sensitive and selective fluorescent detection of 2,4,6-trinitrophenol (TNP). J Mater Chem C 6(41):11162–11169. 10.1039/C8TC04250K
7. Sun RX, Huo XJ, Lu H, Feng SY, Wang DX, Liu HZ (2018) Recyclable fluorescent paper sensor for visual detection of nitroaromatic explosives. Sensor Actuat B-Chem 265:476–487. 10.1016/j.snb.2018.03.072
8. Dong WY, Ma ZH, Duan Q, Fei T (2018) Crosslinked fluorescent conjugated polymer nanoparticles for high performance explosive sensing in aqueous media. Dyes Pigments 159:128–134. 10.1016/j.dyepig.2018.06.018
9. Saumya K, Veettil SC (2019) Fluorene-triazine conjugated porous organic polymerframework for superamplified sensing of nitroaromatic explosives. J Photoch Photobio A 371:414–422. 10.1016/j.jphotochem.2018.11.044
10. Wang S, Liu YH, Yu Y, Du JF, Cui YZ, Song XW, Liang ZQ (2018) Conjugated microporous polymers based on biphenylene for CO_2 adsorption and luminescent detection of nitroaromatic compounds. New J Chem 42:9482–9487. 10.1039/C8NJ01306C
11. Mothika VS, Räupke A, Brinkmann KO, Riedl T, Brunklaus G, Scherf U (2018) Nanometer-thick conjugated microporous polymer films for selective and sensitive vapor-phase TNT detection. ACS Applied Nano Mater 1(11):6483–6492. 10.1021/acsanm.8b01779
12. Yang XL, Hu DY, Chen Q, Li L, Li PX, Ren SB, Bertuzzo M, Chen K, Han DM, Zhou XH, Xia XH (2019) A pyrene-cored conjugated microporous polycarbazole for sensitive and selective detection of hazardous explosives. Inorg Chem Commun 107:107453. 10.1016/j.inoche.2019.107453
13. Geng TM, Zhang C, Chen GF, Ma LZ, Zhang WY, Xia HY (2019) Synthesis of tetraphenylethylene-based fluorescent conjugated microporous polymers for fluorescent sensing and adsorbing iodine. Micropor Mesopor Mat 284:468–475. 10.1016/j.micromeso.2019.04.036
14. Geng TM, Zhu ZM, Wang X, Xia HY, Wang Y, Li DK (2017) Poly{tris[4-(2-Thienyl)phenyl]amine} fluorescent conjugated microporous polymer for selectively sensing picric acid. Sensor Actuat B-Chem 244:334–343. 10.1016/j.snb.2017.01.005
15. Zhang P, Guo J, Wang CC (2012) Magnetic CMP microspheres: multifunctional poly(phenylene ethynylene)frameworks with covalently built-in Fe_3O_4 nanocrystals exhibiting pronounced sensitivity for acetaminophen microdetection. J Mater Chem 22:21426–21433. 10.1039/c2jm34725c
16. Li YK, Bi SM, Liu F, Wu SY, Hu J, Wang LM, Liu HL, Hu Y (2015) Porosity-induced emission: exploring color-controllable fluorescence of porous organic polymers and their chemical sensing applications. J Mater Chem C 3:6876–6881. 10.1039/c5tc00682a

17. Lin GQ, Ding HM, Yuan DQ, Wang BS, Wang C (2016) A Pyrene-based, fluorescent three-dimensional covalent organic framework. J Am Chem Soc 138:3302–3305. 10.1021/jacs.6b00652
18. Gomes R, Bhaumik A (2016) A new triazine functionalized luminescent covalent organic framework for nitroaromatic sensing and CO_2 storage. RSC Adv 6:28047–28054. 10.1039/C6RA01717G
19. Das G, Biswal BP, Kandambeth S, Venkatesh V, Kaur G, Addicoat M, Heine T, Verma S, Banerjee R (2015) Chemical sensing in two dimensional porous covalent organic nanosheets. Chem Sci 6:3931–3939. 10.1039/C5SC00512D
20. Wei F, Cai XY, Nie JQ, Wang FY, Lu CF, Yang GC, Chen ZX, Ma C, Zhang YX (2018) A 1,2,3-triazolyl based conjugated microporous polymer for sensitive detection of p-nitroaniline and Au nanoparticles immobilization. Polym Chem 9(27):3832–3839. 10.1039/C8PY00702K
21. Liu HQ, Wang Y, Mo WQ, Tang HL, Cheng ZY, Chen Y, Zhang ST, Ma HW, Li B, Li XB (2020) Dendrimer-based, high-luminescence conjugated microporous polymer films for highly sensitive and selective volatile organic compound sensor arrays. Adv Funct Mater 1910275 10.1002/adfm.201910275
22. Geng TM, Zhang C, Liu M, Hu C, Chen GF (2020) Preparation of biimidazole-based porous organic polymers for ultrahigh iodine capture and formation of liquid complexes with iodide/polyiodide ions. J Mater Chem A 8:2820–2826. 10.1039/C9TA11982E
23. Deshmukh A, Bandyopadhyay S, James A, Patra A (2016) Trace level detection of nitroanilines using a solution processable fluorescent porous organic polymer. J Mater Chem C 4:4427–4433. 10.1039/C6TC00599C
24. Chen Z, Chen M, Yu YL, Wu LM (2017) Robust synthesis of free-standing and thickness controllable conjugated microporous polymer nanofilms. Chem Commun 53:1989–1992. 10.1039/c6cc09763d

Figures

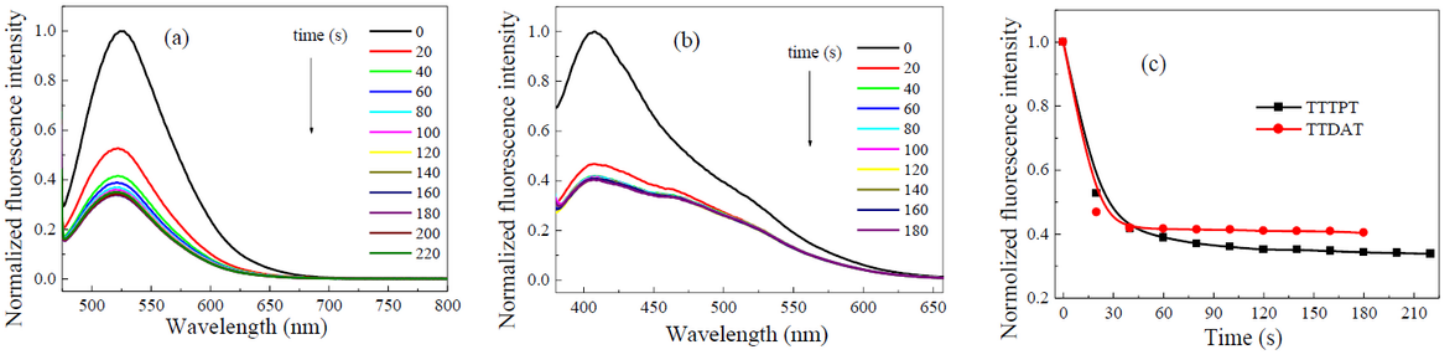

Figure 1

Normalized fluorescence intensities of the CMPs upon addition of TNP (a) TTTPT, (b) TTDAT for different periods of time. (c) The plots of fluorescence maximum of TTTPT and TTDAT as the functions of time (1.0 mg mL-1, TTTPT in DOX: excited at 460 nm; TTDAT in DMF: excited at 350 nm).

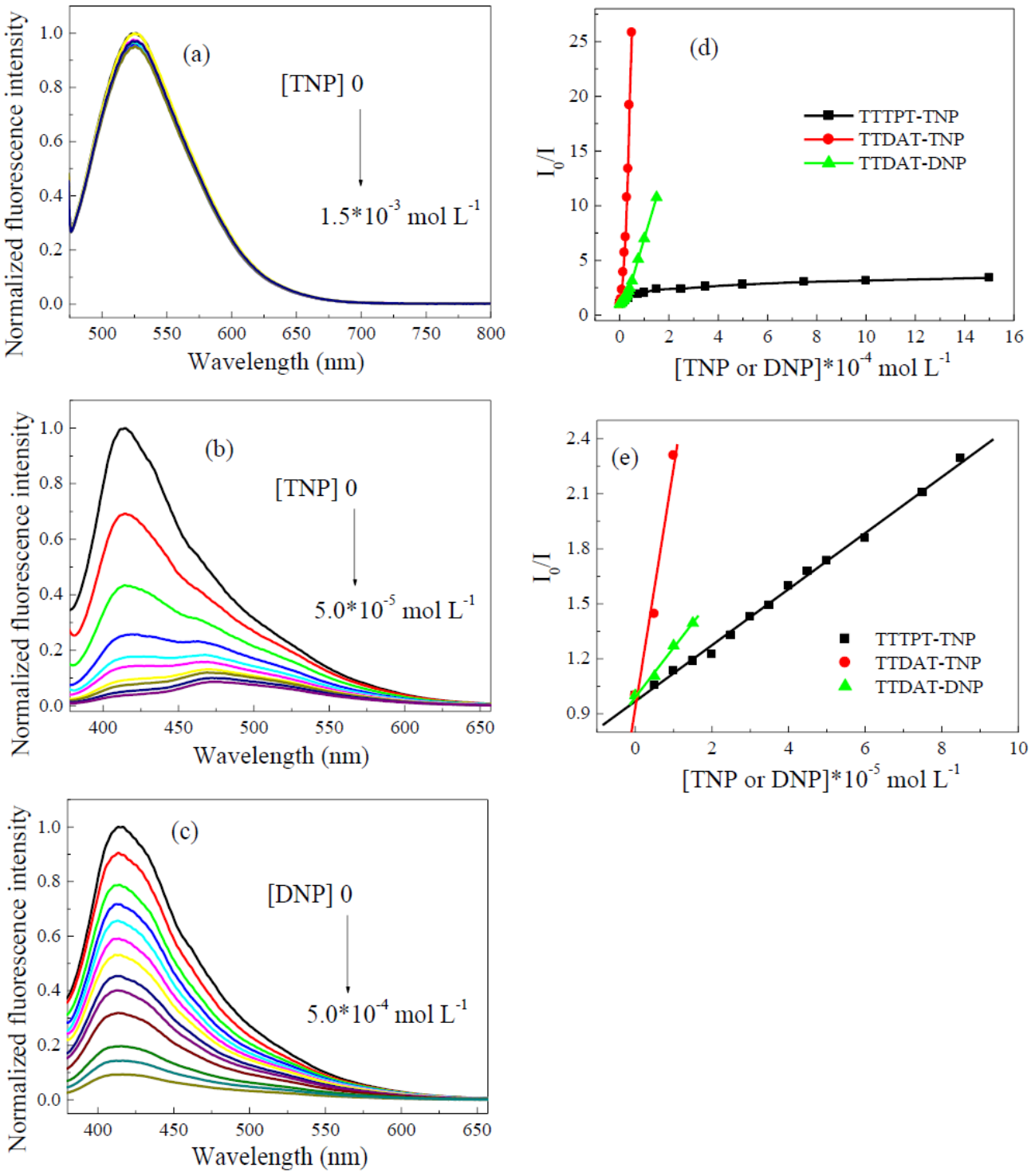

Figure 2

The changes of fluorescence spectra of the (a) TTTPT in dispersions of the DOX upon addition of TNP (1.0 mg mL-1, excited at 460 nm); TTDAT in dispersions of the DMF upon addition of (b) TNP, (c) DNP (1.0 mg mL-1, excited at 350 nm). Relative fluorescence intensity (I0/I) of the (d) TTTPT and TTDAT in dispersions upon addition of various concentrations of TNP or DNP; (e) Stern–Volmer plots of TTTPT and TTDAT with various concentrations of TNP and DNP.

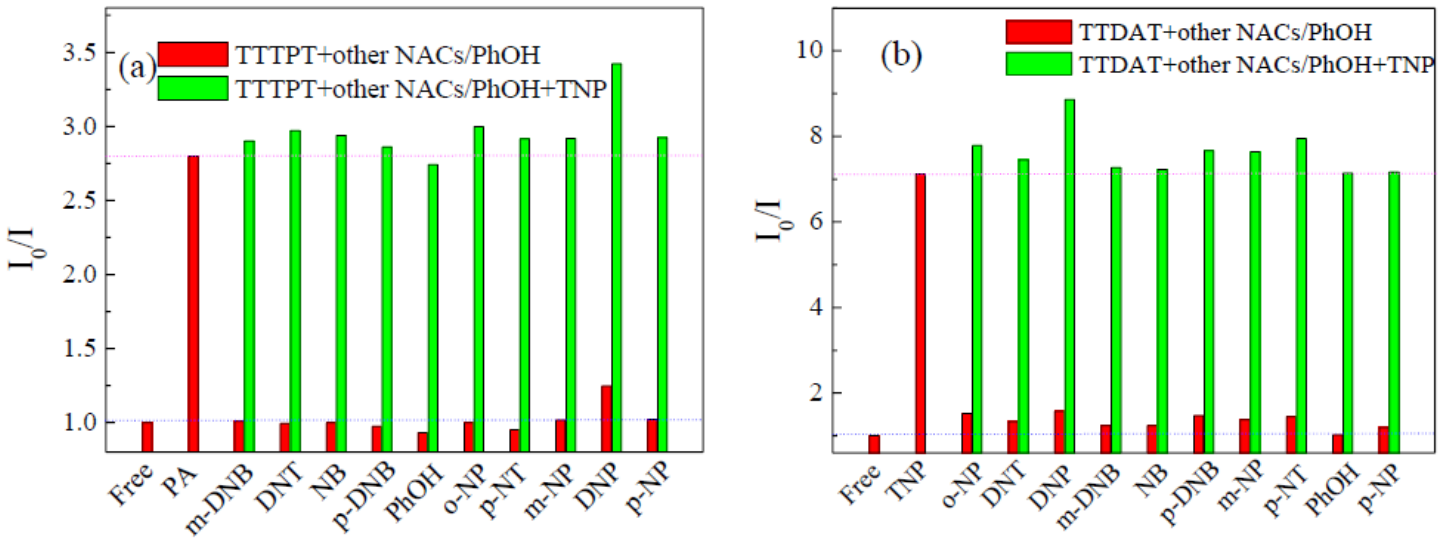

Figure 3

Selectivity and competitiveness of (a) TTTPT in DOX (the concentration of NACs and PhOH: 5.0×10-4 mol L-1, λex =460 nm) toward TNP and (b) of TTDAT in DMF toward TNP (the concentration of NACs and PhOH: 2.5×10-5 mol L-1, λex =350 nm). The red bars represent the relative fluorescent intensities of TTTPT and TTDAT in the presence of the competition NACs and PhOH, and the green bars represent the relative fluorescent intensity upon the addition of TNP to the above solutions.

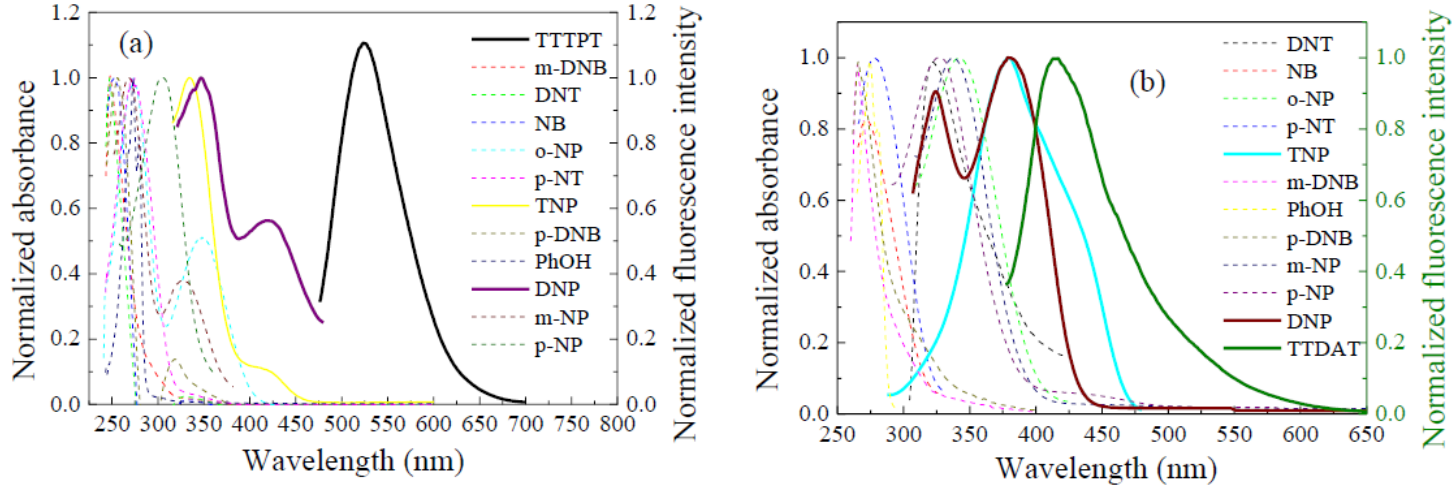

Figure 4

The absorption spectra of DNT, NB, NT, TNP, o-NP, PhOH, m-DNB, p-DNB, DNP, m-NP, p-NP as well as the emission spectra of (a) TTTPT (λex=460 nm, in DOX) and (b) TTDAT (λex=350 nm, in DMF).

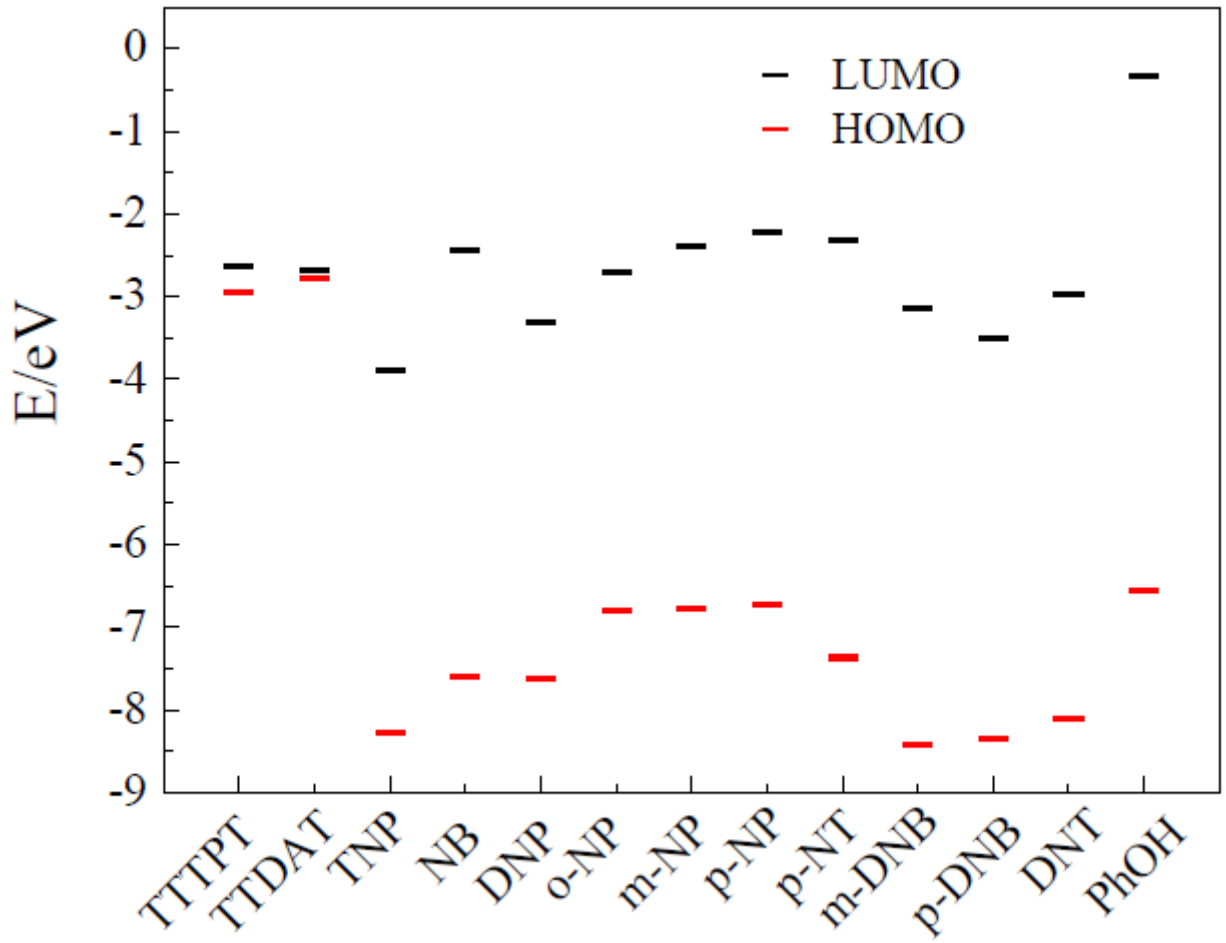

Figure 5

HOMO and LUMO calculations for CMPs, the NACs and PhOH. All the molecular orbital calculations were performed with the Gaussian 09 program at the B3LYP/6-31G* level.

Supplementary Files

This is a list of supplementary files associated with this preprint. Click to download.

- Scheme1.png
- 8.SupplementaryinformationJF.docx